

Fast ray tracing in a cellular model

Lucas Freitas¹ (IC – Unicamp), Jorge Stolfi² (IC – Unicamp), Martin Tygel³ (IMECC – Unicamp)

1 – lucas.batista.freitas@gmail.com

2 – stolfi@ic.unicamp.br

3 – tygel@ime.unicamp.br

We describe a fast method for seismic ray tracing in a cellular model, in which cells can have general polynomial shapes with non-planar bounding faces. The key idea is integration of the ray equations in terms of local cell coordinates rather than spatial coordinates. This approach allows for efficient detection of cell boundary crossing events, suppressing the need for costly non-linear equation solvers in the inner loop.

cellular model, ray tracing, bezier blocks

1 – INTRODUCTION

Seismic simulation is a powerful tool for a number of studies on seismic modeling, imaging and inversion for exploration and monitoring of oil reservoirs. These include, among others, planning of acquisition surveys, image interpretation through identification of key reflections, discrimination of primaries and multiples and amplitude analysis (AVO and AVA).

Among various simulation techniques, ray tracing (Červený (2001)) stands out for its versatility and computational effectiveness. As a consequence, it plays an important role in some more sophisticated simulation methods, such as wavefront construction (see, e.g., Vinje et al., 1999), inversion methods, such as seismic tomography (see e.g., Duvencok, 2004), and others. Kinematic and dynamic ray tracing produce qualitative and quantitative information, namely images, traveltimes, amplitudes and phase shapes that relate various aspects of the wave propagation within the medium under investigation and can, thus, help to understand and interpret the seismic data.

Seismic simulation requires a computer model that captures the geometry of layer structures and interfaces, as well as the lithology of the subsurface region of interest. Subsurface models that are adequate for ray tracing calculations are typically layered structures, which smoothly varying parameters (velocities and density) within the layers. The layer boundaries are typically piecewise smooth surfaces, across which the parameters may have jumps.

Grid-based models, as generally used in tomographic and migration studies, cover the region of interest by a dense uniform grid and assign physical properties to each node of the grid. These models are simple and flexible but space consuming and do not adequately model certain phenomena such as sharp interfaces and narrow intrusions, which are extremely important for seismic ray tracing.

Layer-based models partition the region of interest into layers by surfaces which are modeled as meshes of simple patches (see Gjøystdal et al. (1983)). Layer-based models can naturally represent sharp interfaces but require complex and costly point-mesh location algorithms to detect ray-interface intersections.

Cell-based models partition the region of interest into a number of *blocks*, whose relatively simple geometric shapes are described by a few parameters (see, e.g., Konig, 1995 and Wang, 2000). The shape is usually described by polynomials that map some simple geometric solid to Cartesian space. Ray-interface tests are replaced by simpler tests of a ray against the boundary faces of the current block.

Realistic subsurface models which are suitable for ray tracing must be able to represent interfaces with complex shapes, which considerably increase the difficulty of model construction and seismic simulation. Cell-based models, in particular, require blocks with non-planar faces in order to represent smooth layer interfaces. Ray tracing in such models requires a conversion of Cartesian coordinates to local coordinates to detect the ray intersection with the block boundary. This demands solving a system of polynomial equations, which, in general, requires expensive iterative numerical methods such as Newton or Newton-Raphson (see e.g. Press et al, 1986).

In this paper, we propose a new approach for ray tracing in cell-based models, that guarantees efficient test for boundary crossing detection. The key is performing the ray integration in terms of the block's domain coordinates instead of Cartesian coordinates.

2 – KINEMATIC RAY TRACING

In the high-frequency approximation, the elastodynamic equation produces a non-linear first-order partial differential equation for the travelttime which is usually called the *eikonal equation*. This equation can be written using the Hamiltonian formalism as

$$\mathcal{H}(xc, p) = 0 \quad (1)$$

where \mathcal{H} is the *Hamiltonian function*, $p = \nabla T$ and $T = T(x)$ is the travelttime from the ray's origin to the point x within the subsurface model. Many suitable formulations for \mathcal{H} can be used (see Červený (2001)). The one chosen here is

$$\mathcal{H}(x, p) = \ln(v||p||). \quad (2)$$

Application of *the method of characteristics* (see, e.g. Herzberger,1958) to equation (2) provides three-dimensional trajectories, called *rays*, along which the eikonal equation (1) is satisfied. Each ray is described by the evolution of the *ray state* consisting of a *position function* $x = x(T)$ and a *slowness function* $p = p(T)$ of the time, T , chosen as the running parameter to describe the ray. The slowness vector, p (which, in isotropic media, is orthogonal to the wavefront) is related to the so-called *phase velocity*, $v = v(x)$ by the relationship $|p| = 1/v$. The ray evolution is described by the *characteristic equations* (Herzberger,1958)

$$\frac{dx}{dT} = \nabla_p \mathcal{H} = v^2 p, \quad \frac{dp}{dT} = -\nabla_x \mathcal{H} = -\frac{1}{v} \nabla_x v. \quad (3)$$

Here, we use the notation $\nabla_x = (\partial/\partial x_1, \dots, \partial/\partial x_n)$ and $\nabla_p = (\partial/\partial p_1, \dots, \partial/\partial p_n)$, where n is the dimension of the subsurface model (2 or 3).

The O.D.E. system (3) can, in principle, be numerically solved by any integration method such as Runge-Kutta (Pressman et al., 1986).

Equations (3) are only valid as long as the ray is traveling in a medium where $v(x)$ varies smoothly with x (finite derivatives), which is assumed to be the case within the geological layers. When the ray is about to leave a layer, the intersection point with the layer's boundary must be calculated. At this intersection point, the ray splits into new rays, reflected and/or transmitted. Each new ray changes direction relative to the original ray depending on the ray's angle of incidence at the interface, and the velocity contrast across the interface, according to Snell's law (Červený (2001)). Each new ray is then traced through the next layer. In order to limit the complexity of the simulation, it is general practice to specify the desired wavemodes of the rays along each traversed layer, the so called *signature* of the ray (see Červený (2001)).

3 – GEOLOGICAL MODEL

We assume that the geological model is a partition of space into a finite number of *blocks* or *cells*. Each block is a simple geometric solid (cube, triangular prism or tetrahedron) deformed by polynomial transformations. Adjacent blocks need not share whole faces. Physical properties are assumed to vary smoothly within each block. These concepts are defined formally below

3.1 Simplicies and simploids

We define a *canonical simplex of dimension* $n \geq 0$ as

$$\Delta^n = \{(u_0, \dots, u_n) \in R^{n+1} \mid u_i \geq 0 \wedge \sum_{i=0}^n u_i = 1\} \quad (4)$$

The canonical simplices with dimension 1,2 and 3 are the canonical segment, triangle and tetrahedron, illustrated in figure 1. Note that u_0, \dots, u_n are the *barycentric coordinates* relative to the simplex (see Farin (1992)).

The *canonical simploid of kind* (h_1, \dots, h_k) , denoted by $S^{(h_1, \dots, h_k)}$ is defined as the Cartesian product of simplices $\Delta^{h_1} \times \dots \times \Delta^{h_k}$ (see deRose et al. (1993)). Figure 2 illustrates some simploids.

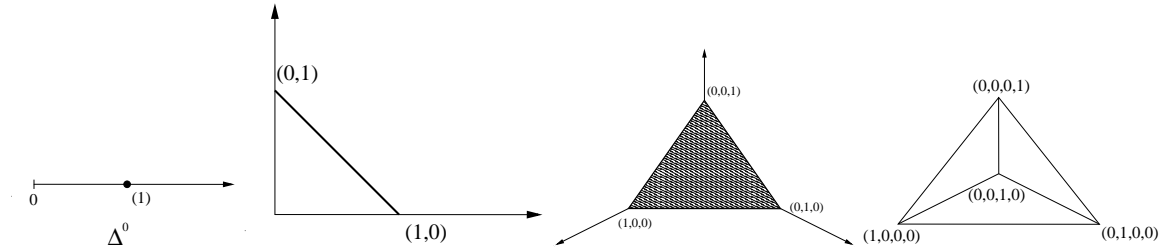


Figure 1: Canonical simplices.

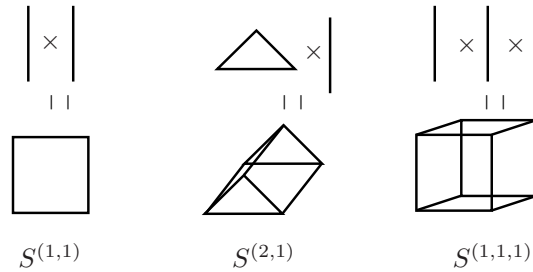


Figure 2: Canonical simplicoids.

3.2 Affine extension of domains

By extending the canonical simplex to include points with negative coordinates we obtain the *affine extension* of Δ^n ; which is the *affine space with dimension n*,

$$A^n = \{u \in R^{n+1} \mid \sum_{i=0}^n u_i = 1\}. \quad (5)$$

Similarly, we define the *affine extension* of a simplicoid $S^{(h_1, \dots, h_k)}$ as the *multi-affine space*

$$A^{h_1, \dots, h_k} = A^{h_1} \times \dots \times A^{h_k}. \quad (6)$$

3.3 Simplicial and simplicoidal polynomials

We say that a function F from A^n to R is a *simplicial polynomial function of degree g* if it is a homogeneous polynomial function of degree g from R^{n+1} to R restricted to A^n .

Let $u^{(1)}, \dots, u^{(k)}$ be points of A^{h_1}, \dots, A^{h_k} , respectively. We define the *i*th *transversal section* of A^{h_1, \dots, h_k} at $u = (u^{(1)}, \dots, u^{(k)}) \in A^{h_1, \dots, h_k}$, denoted by $A^{h_1, \dots, h_k}|_i(u)$, as

$$\{u^{(1)}\} \times \dots \times \{u^{(i-1)}\} \times A^{h_i} \times \{u^{(i+1)}\} \times \dots \times \{u^{(k)}\} \quad (7)$$

Note that there is a bijection from $A^{(h_1, \dots, h_k)}|_i(u)$ to A^{h_i} .

A *simplicoidal polynomial function of type h_1, \dots, h_k and degree $g = (g_1, \dots, g_k)$* is a function F from A^{h_1, \dots, h_k} to R such that when restricted to any transversal section $A^{h_1, \dots, h_k}|_i(u)$, $i \in \{1, \dots, k\}$ equals a simplicial polynomial function of degree g_i from A^{h_i} to R . Note that F cannot, in general, be factored into the product of k simplicial polynomial functions.

3.4 Geophysical block

We define a *geophysical block with n-dimensional domain and m-dimensional range*, or a (n, m) block, as a pair (D, F) where D (the *domain space*) is an n -dimensional canonical simplicoid and F is a simplicoidal polynomial function from \widehat{D} to R^m , where \widehat{D} is the natural extension of D .

3.5 Bézier representation of a block

Let $B = (D, F)$ be a (n, m) -block whose domain D equals $S^{(h_1, \dots, h_k)}$. Observe that the domain is completely defined by the k -uple (h_1, \dots, h_k) . The simplicoidal polynomial function F can be expressed in terms of its *Bézier coefficients* (see deRose et al. (1993)).

In the special case where D is a simplex Δ^n , the representation of F of degree g consists of $f = \binom{g+n}{n}$ Bézier coefficients which are vectors of R^m . We denote these coefficients by c_i where i ranges over I_n^g , the set of all $(n + 1)$ tuples (i_0, \dots, i_n) of natural numbers whose sum is g (see the example in figure 3). The function F can be expressed as

$$F(u) = \sum_{i \in I_n^g} c_i \mathcal{B}_i^{n,g}(u) \quad (8)$$

where $\mathcal{B}_i^{n,g}$ is the *Bernstein-Bézier polynomial of dimension n , degree g and index i* , defined as

$$\mathcal{B}_i^{n,g}(u) = \frac{g!}{i_0! \dots i_n!} u_0^{i_0} \dots u_n^{i_n}.$$

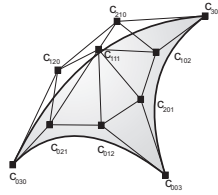


Figure 3: Bézier representation of a $(2, 3)$ -block (D, F) . The domain D is Δ^2 and F has 3 components, X, Y, Z , each a simplicial polynomial of degree 3.

The computation of $F(u)$ by formula (8) can be performed in $\binom{g+n}{n+1}$ n -dimension linear interpolation steps by the DeCastejau algorithm (see Peters (1994)).

Now suppose the domain D is $S^{(h_1, \dots, h_k)}$ and F is a simplicoidal polynomial function of degree $g = (g_1, \dots, g_k)$ (see figure 4). The Bézier representation of F consists of $\prod_{j=1}^k \binom{g_j+h_j}{h_j}$ Bézier coefficients; The value of F at a point $u = (u^{(1)}, \dots, u^{(k)})$ of \hat{D} is given by

$$F(u) = \sum_{i_1 \in I_{h_1}^{g_1}} c_{i_1, \dots, i_k} \mathcal{B}_{i_1}^{g_1, h_1}(u^{(1)}) \dots \mathcal{B}_{i_k}^{g_k, h_k}(u^{(k)}). \quad (9)$$

where c_{i_1, \dots, i_k} are Bézier coefficients.

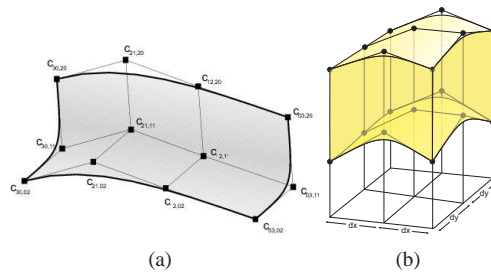


Figure 4: Bézier representation of simplicoidal polynomial functions whose domains are (a) $S^{1,1}$ and (b) $S^{1,1,1}$.

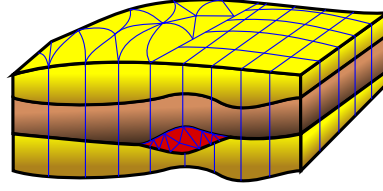


Figure 5: Example of a cellular model.

3.6 Cellular model

For this paper, we define a geophysical model as a collection of (n, m) -blocks whose union covers the region of interest G and whose interiors are disjoint. See figure 5.

The cellular model includes also *topological relations* among blocks (adjacencies, incidences, etc.) which aim to increase the effectiveness of navigation inside the model; and *domain coordinate correspondences* between adjacent blocks. Namely, for each pair of (n, m) -blocks $B' = (D', F')$ and $B'' = (D'', F'')$ that are adjacent through a common face E we store an affine (1st degree) correspondence between the coordinates of \widehat{D}' and \widehat{D}'' . The correspondence is represented by two affine maps Θ' and Θ'' from \widehat{D}' and \widehat{D}'' to R^n such that the images $\Theta'(D')$ and $\Theta''(D'')$ have disjoint interiors but share the face E . Figure 6 illustrates such correspondence.

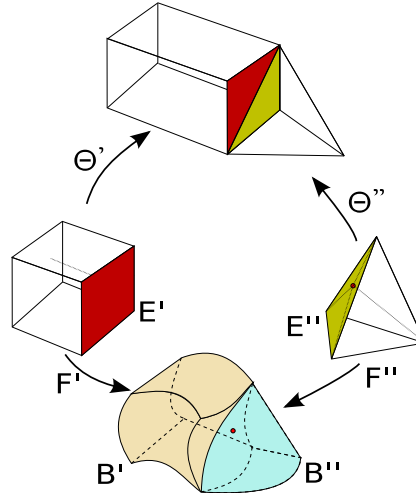


Figure 6: Domain coordinate correspondence.

4 – CELL RAY TRACING IN BLOCKS LOCAL COORDINATES

In our proposed adaptation of ray tracing, the ray equations (3) are expressed and integrated in terms of block's local coordinates (see Figure 7). More precisely, we replace the state $[x, p]$ by $[\alpha, p]$ where α are the local coordinates of the point x in the current block. Note that the slowness vector remains in global (Cartesian) space coordinates.

For this purposes, we define the *simplicial local coordinates* $\alpha = (\alpha_1, \dots, \alpha_n)$ of Δ^n as an arbitrary affine mapping from the affine extension of A^n to R^n . An obvious choice would be $\alpha_i = u_i$ for $i = 1, \dots, n$ (discarding u_0). For a simploid S^{h_1, \dots, h_k} the local coordinates are obtained by concatenating the local coordinates of the constituent simplices $\Delta_{h_1}, \dots, \Delta_{h_k}$.

System (3) is then rewritten as

$$\frac{d\alpha}{dT} = \mathcal{W}^{-1} v^2 p \quad \frac{dp}{dT} = -\mathcal{W}^{-1} \frac{1}{v} \nabla_{\alpha} v \quad (10)$$

where \mathcal{W} is the Jacobian of the block's shape functions.

$$\mathcal{W}_{ij} = \frac{\partial x_i}{\partial \alpha_j} \quad (11)$$

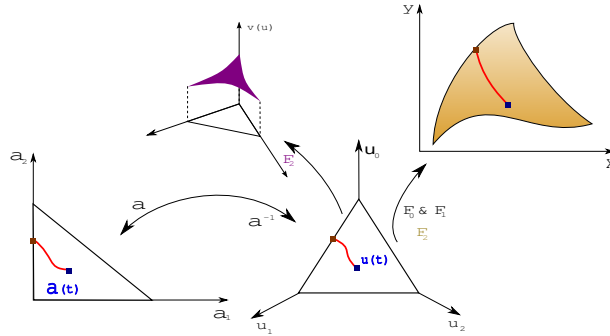


Figure 7: Illustration of parametric ray tracing

The Jacobian \mathcal{W} describes the change from the block’s local coordinates to global Cartesian coordinates. The ∇_{α} operator denotes $(\partial/\partial\alpha_1, \dots, \partial/\partial\alpha_n)$ and ∇_p denotes $(\partial/\partial p_1, \dots, \partial/\partial p_n)$; where n is the domain simploid dimension, and p_i is the i th Cartesian coordinate of the slowness vector p . Each partial derivative is a polynomial simploidal function whose Bézier coefficients are easily and efficiently calculated from the block’s Bézier coefficients.

System (10) is not valid when the matrix \mathcal{W} is singular. However, the absence of such singularities is a basic requirement for a well formed cell-based geomertic model.

The main advantage of this formulation is that detection of the current block limits becomes a set of trivial tests ($\alpha_i = 0$) or 1st degree tests ($\alpha_1 + \dots + \alpha_n = 1$) on the local coordinates.

5 – PHYSICAL PROPERTY MODELLING

The usual approach to modelling space-varying physical properties is what we call *decoupled modelling*. In this approach, space-varying physical properties are specified for each layer by mathematical functions of the Cartesian coordinates (e.g. B-splines) defined over a fixed 3D mesh that is unrelated to the model’s layers and cells. A drawback of this approach is the necessity of a second package of spline/mesh modeling software, with its own data structures, libraries, and editors. Another drawback is that it does not guarantee matching of physical properties with layer shape.

We propose a *coupled model* where the relevant physical properties are modelled by polynomial functions of the domain coordinates inside each block. Typically, for a three-dimensional model, we use $(3, m)$ -blocks with $m > 3$ where the shape of each block (D, F) is described by the first three components of F , while the other $m - 3$ components define the rock’s physical properties. This approach does not require separate data structures, libraries or editors for physical property modelling. Additionally, the unified parameterization ensures a perfect match between shape and properties (see Figure 8).

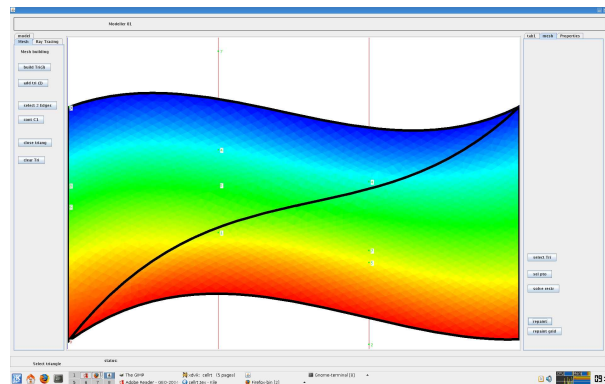


Figure 8: Illustration of a two-dimensional cell-based model with coupled physical modelling. The cells are $(2, 3)$ -blocks whose domains are the canonical triangle $S^{(2)} = \Delta^2$ and whose geometry (black lines) and velocity (color scale) are defined by three simplicial polynomial functions $F(u) = (X(u), Y(u), v(u))$ of degree 3.

Our proposed ray-tracing method is compatible with both approaches for property modelling. Formulation (10) assumes our coupled physical modelling. For the decoupled model, we simply replace $\mathcal{W}^{-1}\nabla_{\alpha}v$ by $\nabla_x v$.

Integration of system (10) requires the evaluation of $d\alpha/dT$ and dp/dT , which, in turn require evaluating v , $\nabla_{\alpha}v$ and the jacobian \mathcal{W} at o point with given local coordinates α . The velocity v can be obtained by applying the DeCasteljau algorithm to the v component of the current block's function F . For the gradient $\nabla_{\alpha}v$, we can precompute the Bézier coefficients of $\partial v/\partial\alpha_1, \dots, \partial v/\partial\alpha_n$ for the current block (Farin (1992)). These derivatives are polynomials of degree $g - 1$ where g is the degree of F . Then, $\nabla_{\alpha}v$ can be computed for any given α by n applications of DeCasteljau. The Jacobian element \mathcal{W}_{ij} can be computed in the same way, from the Bézier coefficients of the X, Y, Z components of F .

Observe that the computation of the Jacobian \mathcal{W}_{ij} and of the products $\mathcal{W}_{ij}^{-1}\nabla_{\alpha}v$ and $\mathcal{W}_{ij}^{-1}v^2p$ does not require iteration or recursive subdivision, and is therefore faster in general than the ray-boundary tests that are eliminated by our ray tracing approach.

6 – NUMERICAL EXAMPLE

As an example, consider ray tracing in the two-dimensional geophysical model shown in Figure 9, which has the same cell type and physical modelling as Figure 8. Figure 10 shows the results of tracing a fan of rays from the upper left corner with a fourth-order Runge-Kutta integrator (Press et al. (1986)). The initial ray direction varied from 5° to 85° in 5° increment. The ray position $X(T)$ was sampled at each 2ms,

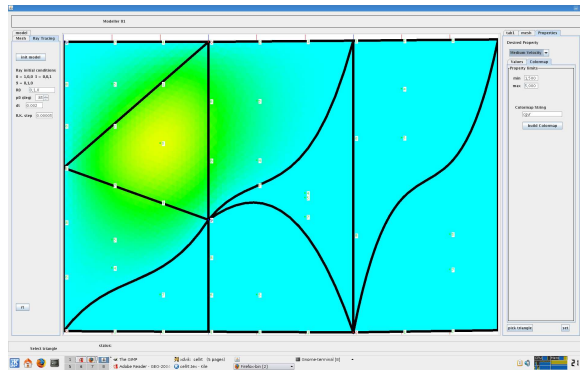


Figure 9: Velocity model used in Figure 10. The velocity range is from 1500m/s (cyan) to 5000m/s (red).

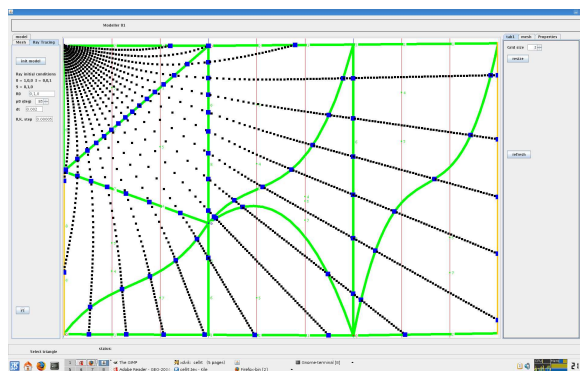


Figure 10: Propagation of a fan of rays in the proposed cellular model.

7 – CONCLUSIONS AND FUTURE WORK

Integrating ray equations in terms of local coordinates (equation (10)) reduces considerably the cost of boundary tests when integrating the ray propagation O.D.E. We plan further improvements by detecting whether system (10) has analytical solution in the current block, which would allow us to cross that block in a single step.

8 – ACKNOWLEDGMENTS

We acknowledge support by FAPESP (grant 06/50344-4), CNPq (grant 301016/92-5) and the WIT Consortium.

REFERENCES

- deROSE, T.D., GOLDMAN, R.N., HAGEN, H. and MANN, S. Functional composition algorithms via blossoming. **ACM Transactions on Graphics**, v. 12, no. 2, 1993.
- DUVENECK, E. 3-D tomographic velocity model estimation with kinematic wavefield attributes. **Geophysical Prosp**, v. 52, no. 6, p. 535–545, 2004.
- FARIN, G. Curves and Surfaces for Computer Aided Geometric Design. **Academic Press** 1992.
- GJØYSTDAL, H. , REINHARDSEN, J.E., ÅSTEBØL, A. Computer representation of complex 3-D geologic structures using a new “Solid Modeling” technique. **SEG Technical Program Expanded Abstracts**
- KONIG, M. Cell ray tracing for smooth, isotropic media: a new concept based on a generalized analytic solution **Geophysical Journal International**, 1995.
- PETTERS, J. Evaluation and approximate evaluation of the multivariate Bernstein-Bézier form on a regularly partitioned simplex *ACM Trans. Math Softw*, v 20, p. 460–480, 1994.
- PRESS, W.H., FLANNERY, B. p., TEUKOLSKY, S.A., VETTERLING, W.T *Numerical Recipes* **Cambridge University Press**, 1986
- ČERVENÝ, V *Seismic Ray Theory* **Cambridge University Press**
- VINJE, V., IVERSEN, E., GJØYSTDAL, H., ÅSTEBØL 3D Ray Modeling by Wavefront Construction in Open Models **Geophysics**, v. 64, no. 6, p. 1912–1919,
- WANG, L Estimation of Multi-valued Green’s function by Dynamic Ray tracing and True Amplitude Kirchoff Inversion in 3D-Heterogeneous media **Phd Thesis**, CWP